AMERICAN SOCIETY FOR MICROBIOLOGY | Infection and Immunity

The Tick Protein Sialostatin L2 Binds to Annexin A2 and Inhibits NLRC4-Mediated Inflammasome Activation

Xiaowei Wang,[a] Dana K. Shaw,[a] Olivia S. Sakhon,[a]* Greg A. Snyder,[b] Eric J. Sundberg,[c] Laura Santambrogio,[d] Fayyaz S. Sutterwala,[e] J. Stephen Dumler,[a,f] Kari Ann Shirey,[a] Darren J. Perkins,[a] Katharina Richard,[a] Andrezza C. Chagas,[g] Eric Calvo,[g] Jan Kopecký,[h] Michail Kotsyfakis,[i] Joao H. F. Pedra[a]

Department of Microbiology and Immunology, University of Maryland School of Medicine, Baltimore, Maryland, USA[a]; Institute of Human Virology, Department of Medicine, University of Maryland School of Medicine, Baltimore, Maryland, USA[b]; Institute of Human Virology, Departments of Medicine and Microbiology and Immunology, University of Maryland School of Medicine, Baltimore, Maryland, USA[c]; Departments of Pathology, Microbiology and Immunology and Orthopedic Surgery, Albert Einstein College of Medicine, Yeshiva University, Bronx, New York, USA[d]; Inflammation Program and Division of Infectious Diseases, Department of Internal Medicine, University of Iowa, Iowa City, Iowa, USA[e]; Department of Pathology, University of Maryland School of Medicine, Baltimore, Maryland, USA[f]; Laboratory of Malaria and Vector Research, National Institute of Allergy and Infectious Diseases, National Institutes of Health, Rockville, Maryland, USA[g]; Faculty of Science, University of South Bohemia in České Budějovice, Budweis, Czech Republic[h]; Institute of Parasitology, Biology Centre, Czech Academy of Sciences, Budweis, Czech Republic[i]

Tick saliva contains a number of effector molecules that inhibit host immunity and facilitate pathogen transmission. How tick proteins regulate immune signaling, however, is incompletely understood. Here, we describe that loop 2 of sialostatin L2, an anti-inflammatory tick protein, binds to annexin A2 and impairs the formation of the NLRC4 inflammasome during infection with the rickettsial agent *Anaplasma phagocytophilum*. Macrophages deficient in annexin A2 secreted significantly smaller amounts of interleukin-1β (IL-1β) and IL-18 and had a defect in NLRC4 inflammasome oligomerization and caspase-1 activation. Accordingly, *Annexin a2*-deficient mice were more susceptible to *A. phagocytophilum* infection and showed splenomegaly, thrombocytopenia, and monocytopenia. Providing translational support to our findings, better binding of annexin A2 to sialostatin L2 in sera from 21 out of 23 infected patients than in sera from control individuals was also demonstrated. Overall, we establish a unique mode of inflammasome evasion by a pathogen, centered on a blood-feeding arthropod.

Ticks are obligate blood-feeding arthropods that transmit a multitude of infectious agents, including viruses, bacteria, fungi, protozoa, and helminths (1–3). Pathogen transmission occurs during the uptake of a blood meal, when ticks inject saliva into the mammalian host, affecting hemostasis and host immune responses (1–3). Tick saliva contains an arsenal of molecules with antihemostatic, anesthetic, and anti-inflammatory properties (4–6). How tick salivary proteins manipulate the activity of the inflammasome remains mostly elusive. Inflammasomes are complex structures that orchestrate the maturation of the proinflammatory cytokines interleukin-1β (IL-1β) and IL-18 (7–9). Inflammasomes are categorized according to their cognate Nod-like receptor (NLR) member and lead to the activation of caspase-1 and -11 (caspase-4 in humans) (7–9). Activated caspase-1 then processes pro-IL-1β and pro-IL-18 into their mature forms (7), promoting host defenses through complex pleiotropic mechanisms (7–9).

The NLRC4 inflammasome is activated in response to components of the bacterial type III secretion system and flagellin (8–11). To sense virulent bacteria, NLRC4 cooligomerizes with ancillary molecules referred to as NAIPs (neuronal apoptosis inhibitory proteins) (8, 9). NAIP5 and NAIP6 directly bind flagellin, whereas NAIP2 and NAIP1 (human NAIP) recognize the bacterial type III secretion system rod and the needle protein that trigger NLRC4 activation (12–15). Previously, we demonstrated that the tick salivary protein sialostatin L2 targets inflammasome activity during host stimulation with the rickettsial bacterium *Anaplasma phagocytophilum*, the causative agent of human granulocytic anaplasmosis (16). Which protein was binding to sialostatin L2 and whether this molecule affected inflammasome activation during rickettsial infection remained unclear.

In this report, we reveal that sialostatin L2 impairs the formation of the NLRC4 inflammasome during rickettsial infection. The inhibition of NLRC4 inflammasome activity occurs because sialostatin L2 tethers to the phospholipid binding protein annexin A2 in both animal models and patients, hence blocking NLRC4 inflammasome oligomerization, caspase-1 activation, and IL-1β and IL-18 secretion. Given the importance of the inflammasome for pathogen recognition, our findings provide a novel facet for the understanding of arthropod-borne diseases.

MATERIALS AND METHODS

Mice, bacteria, and cell cultures. Breeding and experiments were performed in strict compliance with guidelines set forth by the National Institutes of Health (Office of Laboratory Animal Welfare [OLAW] assurance number A3200-01). Procedures were approved by the Institutional Biosafety Committee (IBC) (approval number 00002247) and the Insti-

Received 18 December 2015 **Returned for modification** 25 January 2016
Accepted 28 March 2016

Accepted manuscript posted online 4 April 2016

Citation Wang X, Shaw DK, Sakhon OS, Snyder GA, Sundberg EJ, Santambrogio L, Sutterwala FS, Dumler JS, Shirey KA, Perkins DJ, Richard K, Chagas AC, Calvo E, Kopecký J, Kotsyfakis M, Pedra JHF. 2016. The tick protein sialostatin L2 binds to annexin A2 and inhibits NLRC4-mediated inflammasome activation. Infect Immun 84:1796–1805. doi:10.1128/IAI.01526-15.

Editor: C. R. Roy, Yale University School of Medicine

Address correspondence to Joao H. F. Pedra, jpedra@som.umaryland.edu.

* Present address: Olivia S. Sakhon, Division of Biomedical Sciences, University of California, Riverside, School of Medicine, Riverside, California, USA.

Supplemental material for this article may be found at http://dx.doi.org/10.1128/IAI.01526-15.

tutional Animal Care and Use Committee (IACUC) (approval number 0413017) at the University of Maryland, Baltimore. C57BL/6 mice (catalog number 000664) were purchased from Jackson Laboratories. *Caspase-11*$^{-/-}$ and *Annexin a2*$^{-/-}$ mice were gifts from Vishva Dixit (Genentech) and Katherine Hajjar (Weill Cornell Medical College). *Nlrc4*$^{-/-}$, *Caspase-1/11*$^{-/-}$, *Myd88*$^{-/-}$, and *Annexin a2*$^{-/-}$ mice were previously described (17, 18). Mice were gender matched and at least 6 to 10 weeks of age. Bone marrow-derived macrophages (BMDMs) were generated as previously described (16). Culturing of *A. phagocytophilum* strain HZ and calculations were described previously (16). Both *Salmonella enterica* serovar Typhimurium strain SL1344 and the *Francisella tularensis* live vaccine strain (LVS) were a gift from Stefanie Vogel at the University of Maryland, Baltimore, School of Medicine. *Francisella* LVS bacteria were grown on cysteine heart agar (Difco) supplemented with 5% horse blood cells at 37°C. Isolates were inoculated in Mueller-Hinton broth (Difco) supplemented with 2% (wt/vol) IsoVitaleX, 1% (wt/vol) glucose, and 0.25% (wt/vol) ferric pyrophosphate. *Salmonella* bacteria were grown in HS medium at 37°C and enumerated as previously described (19).

Patients. Human clinical serum samples were obtained over a range of years from 1994 through 2013 under Institutional Review Board (IRB) protocols approved at the Duluth Clinic (Minnesota) and through IRB-approved exemptions for their use at the University of Maryland, Baltimore, School of Medicine and The Johns Hopkins University School of Medicine (approval number 01-03-26-04e). Samples approved at the Duluth Clinic required consent to obtain serum and blood during the acute and the convalescent phases of infection. The IRB protocol was registered under the protocol "Molecular and Antigenic Study of a Novel Human *Ehrlichia*" on 11 February 1994. The second protocol was approved under an exempt status by the University of Maryland, Baltimore, School of Medicine on 21 February 1994 for the use of the prospectively obtained samples from the Duluth Clinic. The third protocol was approved by The Johns Hopkins University School of Medicine in January 1996 and received an exemption from the Joint Committee on Clinical Investigation.

Chemical reagents. Lipopolysaccharide (LPS) was purchased from InvivoGen. Nigericin and ATP were purchased from Sigma-Aldrich. Recombinant human annexin A2 was purchased from Abcam and Novus Biologicals. Bovine serum albumin (BSA) was purchased from New England BioLabs.

Sialostatin L2 cloning, protein expression, peptides, and antibodies. Full-length sialostatin L2 from the tick *Ixodes scapularis* was amplified by PCR from the clone pET-17b-Sialostatin L2 with forward (Fwd) primer 5′-GGCCGGATCCGAACTGGCTCTGCGTGGTGG-3′ and reverse (Rev) primer 5′-GGCCCTCGAGTTTATGCGGCCGCACACTCAA-3′ containing BamHI and XhoI sites, respectively (underlined). The amplicon was digested and cloned into pGEX-6-P2 (GE Healthcare). Results of sequencing analysis were verified by using pGEX primers (Fwd primer 5′-GGGCTGGCAAGCCACGTTTGGTG-3′/Rev primer 5′-CCGGGAGCTGCATGTGTCAGAGG-3′) at the University of Maryland, Baltimore, Biopolymer Core Facility. A glutathione *S*-transferase (GST)–sialostatin L2 fusion protein was induced and purified in *Escherichia coli* BL21(DE3) cells. Endotoxin-free recombinant sialostatin L2 (rSL2) and the three sialostatin L2 peptides were produced as previously described (16). The amino acid sequences of the three synthesized peptides were (i) ELALRGGYRERSNQDDPEY for the N terminus, (ii) SAQQPGKTHFDTVVEVLKVETQTVAGT for loop 1, and (iii) TCELTSTYNKDTCQANANAAQRTCTTVIYRNLQGEKSISSFECAA for loop 2. Peptide synthesis and folding were performed by an external contractor (SynBioSci Corporation).

GST or the recombinant GST-sialostatin L2 proteins were purified by using GST-Bind resin (Thermo Scientific) according to the manufacturer's instructions. Purified proteins were dialyzed with 10 mM Tris-HCl buffer (pH 7.5) using SnakeSkin dialysis tubing (3,500-molecular-weight [3.5K] cutoff; Thermo Scientific) and were concentrated with centrifuge filter units (3K cutoff; Amicon). The protein concentration was determined by using the bicinchoninic acid (BCA) assay (Thermo Scientific). Sialostatin L2 mouse monoclonal and rabbit polyclonal antibodies were produced at the Institute of Parasitology, Biology Centre, Academy of Sciences of the Czech Republic. Sialostatin L2 rabbit polyclonal antibody was purified with a Melon Gel IgG Spin Purification kit (Thermo Scientific). Normal rabbit IgG was purchased from Santa Cruz. For the monoclonal sialostatin L2 antibody, a BALB/c mouse was immunized intraperitoneally with three doses containing 10 μg each of sialostatin L2 14 days apart. The first dose was administered with complete Freund's adjuvant (Sigma), the second was administered with incomplete Freund's adjuvant (Sigma), and the third was administered without adjuvant 3 days before fusion. Spleen cells were fused with Sp2/0 myeloma cells by using polyethylene glycol (Sigma). Hybridoma cells were cloned by a limiting-dilution technique. Antibodies in hybridoma culture medium were detected by an indirect enzyme-linked immunosorbent assay (ELISA). Monoclonal antibodies were purified from culture medium by using a Montage antibody purification kit with Prosep-A medium (Millipore).

GST pulldown assays. A total of 1.25 nM GST or GST-sialostatin L2 was incubated with equilibrated GST-Bind resin (Thermo Scientific) for 1 h at 4°C. After five washes with the GST binding/washing buffer (25 mM Tris and 150 mM NaCl [pH 7.3]), the resin was incubated with 1 mg of BMDM lysates infected with *A. phagocytophilum* for 1 h at 4°C. Following seven washes with modified GST binding/washing buffer containing 200 mM NaCl, the protein complexes were cleaved from GST resin with GST PreScission protease (GE HealthCare). Eluates were identified by the proteomics facility of the University of Maryland, Baltimore, School of Pharmacy.

Native polyacrylamide gel electrophoresis. Equal amounts of supernatants were mixed with native sample buffer (62.5 mM Tris-HCl, 40% glycerol, 0.01% bromophenol blue [pH 6.8]), loaded into 4 to 15% Mini-Protean TGX precast gels, and run at 200 V for 2 h in 1× Tris-glycine native running buffer (25 mM Tris, 192 mM glycine [pH 8.3]). A NativeMark unstained protein standard (Invitrogen) was visualized with Gel Code Blue Safe Protein Stain solution (Thermo Scientific).

Immunoblotting. Cell lysates were prepared in radioimmunoprecipitation assay (RIPA) lysis buffer (Boston Bioproducts) with Halt protease inhibitor cocktail (Thermo Scientific) and PhosSTOP (Roche Applied Science). Four percent to 15% Mini-Protean TGX precast gels were run at 200 V for 30 min in 1× Tris-glycine-SDS running buffer (Boston Bioproducts). Transfer was performed by using Bio-Rad Trans-Blot Turbo with either polyvinylidene difluoride (PVDF) or nitrocellulose membranes (Bio-Rad). Membranes were blocked in 5% skim milk or BSA (Bio-Rad). Western blot antibodies for caspase-1 (1:1,000 [catalog number 06-503 or 06-503-I; Millipore], 1:2,000 [catalog number 4175, cell line 4B4.2.1; Genentech], or 1:1,000 [catalog number AG-20B-0042; AdiPoGen International]), NLRC4 (1:1,000) (catalog number 06-1125; Millipore), IL-1β (1:1,000) (catalog numbers AF401-NA [R&D Systems] and 12426S [Cell Signaling]), IL-18 (1:1,000) (catalog number JM-5180-100; MBL), β-actin (1:1,000) (catalog number A2103; Sigma), annexin A2 (1:1,000) (catalog numbers 60051-1-1g [Protein Tech] and PA1-9006 [Thermo Scientific]), anti-mouse horseradish peroxidase (HRP), anti-goat HRP, anti-rabbit HRP (1:5,000) (catalog numbers ab97046, ab97110, and ab97051, respectively; Abcam), and anti-rat (1:5,000) (catalog numbers ab97057 [Abcam] and sc-2006 [Santa Cruz Biotechnology]) were used. The enhanced chemiluminescence (ECL) Western blotting substrate and Super Signal West Pico chemiluminescent substrate were used (Thermo Scientific). Restore Western blot stripping buffer was used for the stripping of antibodies on the blots (Thermo Scientific).

ELISAs and binding assays. IL-1β and IL-6 levels were measured with the BD OptEIA set (BD Biosciences). IL-18 capture (1:1,000) (catalog number D047-3) and detection (1:2,000) (catalog number D048-6) antibodies were purchased from MBL. For binding assays, C57BL/6 BMDMs were lysed in RIPA buffer supplemented with Halt protease inhibitor cocktail (Thermo Scientific) and PhosSTOP (Roche Applied Science). Ninety-six-well plates were coated with 0.5 μg of the cell lysate resuspended in 0.5 M carbonate-bicarbonate (pH 9.5) at 4°C overnight. Plates

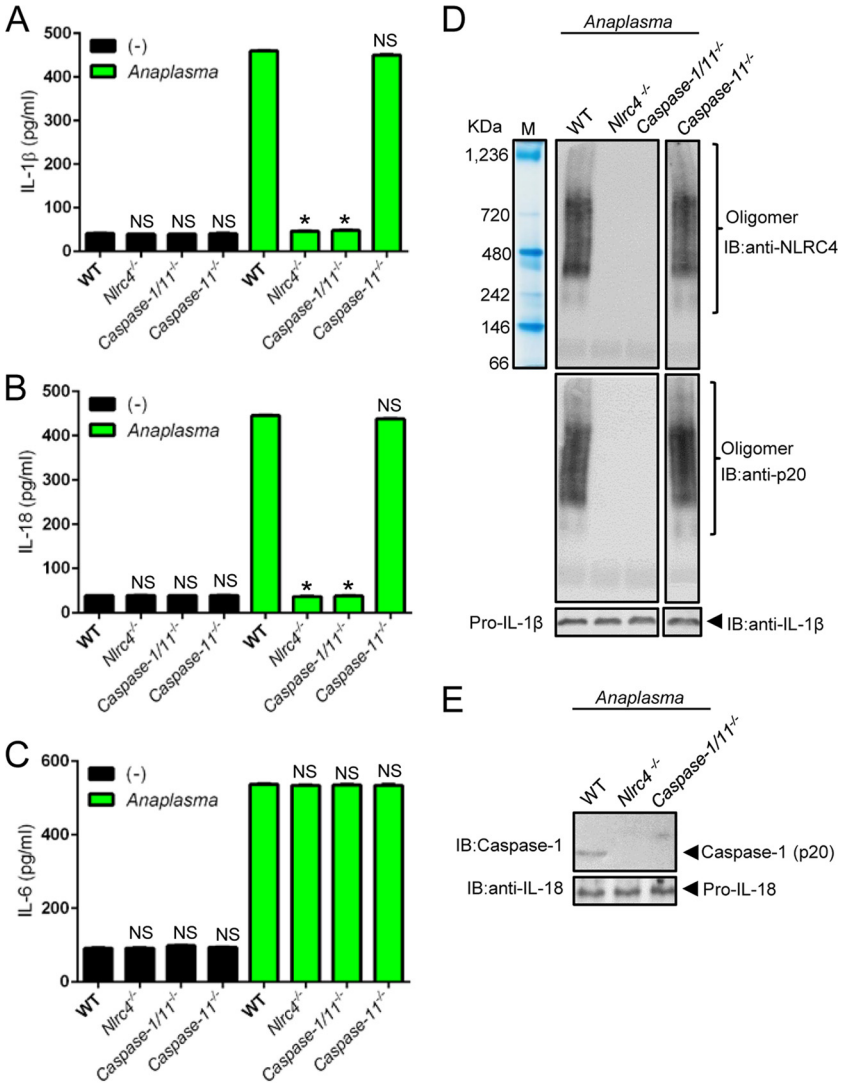

FIG 1 *A. phagocytophilum* induces the NLRC4 inflammasome pathway. BMDMs from wild-type (WT) and deficient mice were stimulated with *A. phagocytophilum* (MOI of 50). (A to C) Levels of IL-1β (A), IL-18 (B), and IL-6 (C) release were measured by an ELISA. (D) Native gel electrophoresis followed by immunoblotting (IB) of NLRC4 and caspase-1 (p20). (E) Caspase-1 autoproteolysis (p20) in macrophages activated upon *A. phagocytophilum* infection. Pro-IL-1β and pro-IL-18 were detected in cell lysates. −, nonstimulated; M, marker. *, $P < 0.05$; NS, nonsignificant (as determined by one-way ANOVA-Dunnett test).

were washed (1× phosphate-buffered saline [PBS], 0.05% Tween 20) and blocked with assay diluent (1× PBS, 10% heat-inactivated fetal bovine serum [FBS]) for 1 h at room temperature, followed by incubation with the polyclonal sialostatin L2 antibody (1:200) and the goat anti-rabbit IgG-HRP-conjugated antibody (1:10,000) (Abcam). A 1:1 mixture of the 3,3′,5,5′-tetramethylbenzidine (TMB) substrate (BD Biosciences) was made and added to each well. Plates were incubated for up to 30 min before the reaction was stopped with 1 M H_2SO_4. The Bio-Rad iMark reader was used to measure the absorbance at 450 nm with a 595-nm correction.

To detect the binding specificity of the sialostatin L2 monoclonal or polyclonal antibody, 0.2 μg of the recombinant sialostatin L2 protein was coated in 0.5 M carbonate-bicarbonate coating buffer and incubated with antibodies at the indicated concentrations. For the detection of protein interactions, C57BL/6 and *Annexin a2*$^{-/-}$ BMDMs treated with *A. phagocytophilum* (multiplicity of infection [MOI] of 50) were lysed as described above and incubated with different titrations of mouse sialostatin L2 monoclonal antibody with 5 μM sialostatin L2 for 2 h at room temperature. The rabbit affinity-purified sialostatin L2 polyclonal antibody (1:200) and goat anti-rabbit IgG-HRP (1:10,000; Abcam) were used for the detection of protein complexes. In the converse binding experiments, annexin A2 polyclonal antibody derived from goat (1:200; Thermo Scientific) and donkey anti-goat IgG-HRP (1:10,000; Abcam) were used.

Quantitative RT-PCR. Genomic DNA from mice was isolated with a DNeasy blood and tissue kit (Qiagen). Quantitative reverse transcription-PCR (RT-PCR) was performed by using Power SYBR green PCR master mix (Invitrogen) in an ABI 7500 real-time PCR instrument. Primer sequences for *A. phagocytophilum* were as follows: 16S-F (5′-CAGCCACA CTGGAACTGAGA-3′) and 16S-R (5′-CCCTAAGGCCTTCCTCACTC-3′). Gene expression was normalized by using primers β-actin-F (5′-ACGCAGAGGGAAATCGTGCGTGAC-3′) and β-actin-R (5′-ACGCG GGAGGAAGAGGATGCGGCAGTG-3′). The absolute quantification method was used.

Mobility shift electrophoresis. A total of 0.2 μg of annexin A2 was mixed with different amounts of recombinant sialostatin L2 as indicated, followed by native PAGE and immunoblotting assays with the anti-an-

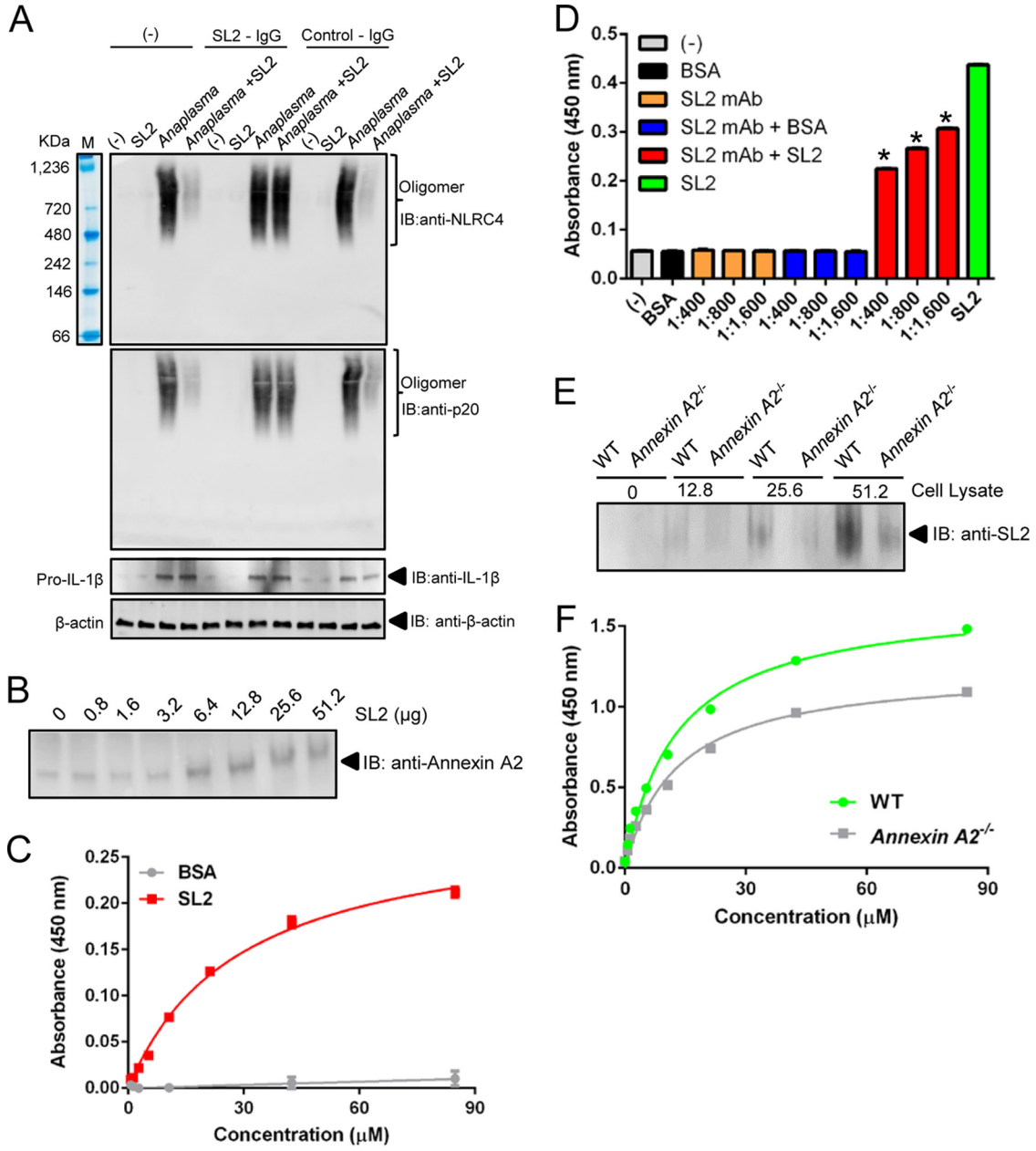

FIG 2 Annexin A2 binds to sialostatin L2. (A) BMDMs were pretreated for 30 min with sialostatin L2 (5 μM), sialostatin L2-IgG (10 ng/μl), and control IgG (10 ng/μl) polyclonal antibodies prior to *A. phagocytophilum* infection. Shown are native gels and immunoblots (IB) of NLRC4 and caspase-1 (p20). β-Actin and pro-IL-1β were detected in cell lysates. −, nonstimulated; M, marker. (B and C) Annexin A2 (0.2 μg)/sialostatin L2 mobility electrophoresis/immunoblotting and ELISAs. (D) Sialostatin L2/annexin A2 inhibition by a monoclonal antibody (mAb). (E and F) Sialostatin L2 incubated with cell lysates followed by native gel electrophoresis/sialostatin L2 immunoblotting or an ELISA. *, $P < 0.05$.

nexin A2 mouse monoclonal antibody (1:500; Protein Tech) and goat anti-mouse HRP (1:5,000; Abcam). A total of 1.0 μg of recombinant sialostatin L2 was mixed with different amounts of either C57BL/6 or *Annexin a2*-deficient BMDM lysates.

Structural docking analysis. Docking of sialostatin L2 (PDB accession number 3LH4) into the human annexin A2 protein (PDB accession number 2HYW) was performed by using the programs GRAMMX (20) and ZDOCK 3.0.2 (21). All residues were included in docking algorithms with no bias defined for either crystal structure. The program PyMOL (22) was used to generate a cartoon representation of the docked structures.

***In vivo* infection.** C57BL/6 ($n = 20$) and *Annexin a2*$^{-/-}$ ($n = 11$) mice were infected by intraperitoneal injection with *A. phagocytophilum* strain HZ (1×10^7 cells). Blood samples were collected at days 0, 5, and 10 for the IL-18 ELISA. Spleens were removed, normalized to body weight, and compared to those of noninfected mice. Spleens were fixed at day 15 postinfection with 10% neutral buffered formalin and embedded in paraffin wax. Sections (5 μm) were obtained and stained with hematoxylin and eosin. Measurement of the *A. phagocytophilum* load was done at day 5 postinfection in the peripheral blood of infected animals by using quantitative RT-PCR, as described above. Numbers of platelets and monocytes were measured at day 15 postinfection in a commercial laboratory (Antech Diagnostics).

Statistical analysis. All experiments in this study were performed with at least 2 to 5 replicates. All data were expressed as means ± standard

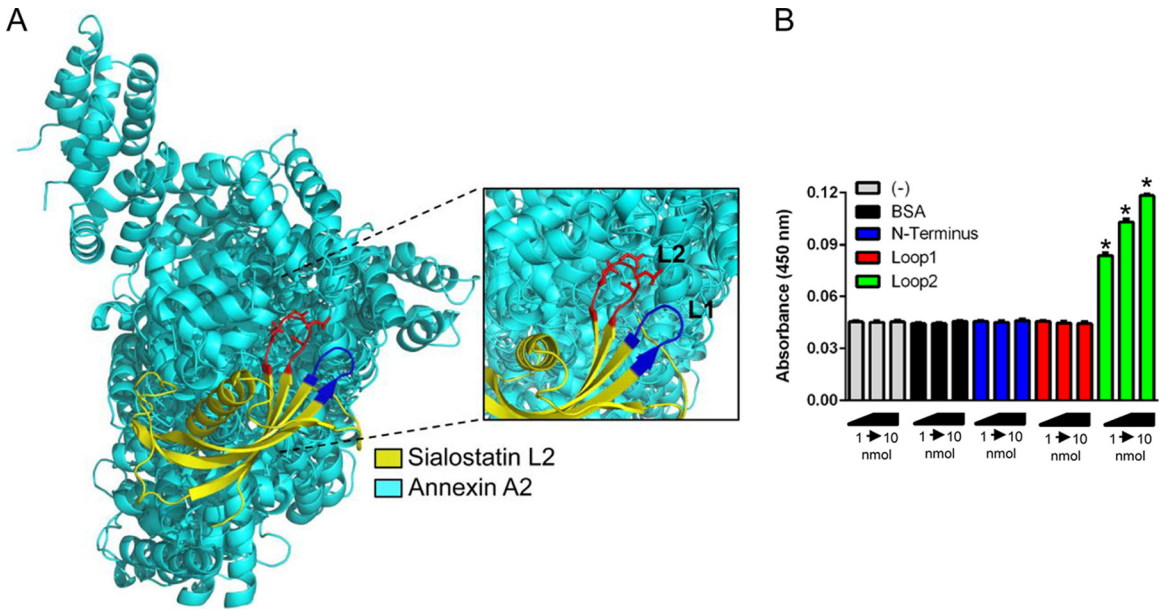

FIG 3 The loop 2 region of sialostatin L2 binds to annexin A2. (A) Docking of sialostatin L2 (PDB accession number 3LH4) bound to annexin A2 (PDB accession number 2HYW). L2, loop 2 (red); L1, loop 1 (dark blue). (B) Annexin A2 (0.2 μg) bound to loop 2. *, $P < 0.05$, as determined by one-way ANOVA-Tukey test.

errors of the means (SEM). The differences between groups were examined by either unpaired Student's *t* test or one-way analysis of variance (ANOVA). All statistical calculations and graphs were made by using GraphPad Prism version 6.0. A *P* value of <0.05 was considered statistically significant.

RESULTS AND DISCUSSION

The NLRC4 inflammasome is activated during *A. phagocytophilum* infection. We previously reported that mice deficient in *Nlrc4* and *Caspase-1/11* are susceptible to *A. phagocytophilum* infection (17). To provide support for this concept, we first stimulated unprimed murine bone marrow-derived macrophages (BMDMs) with *A. phagocytophilum*. Wild-type macrophages secreted IL-1β and IL-18 upon stimulation (Fig. 1A and B), while *Nlrc4*$^{-/-}$ and *Caspase-1/11*$^{-/-}$ macrophages exhibited severe defects in IL-1β and IL-18 release (Fig. 1A and B). As expected, secretion of IL-6 and translation of IL-1β and IL-18 by macrophages, which are not regulated by the inflammasome, remained unaffected (Fig. 1C to E). Oligomerization of the inflammasome (Fig. 1D) and caspase-1 autoproteolysis (Fig. 1E) were hindered in the absence of NLRC4 and caspase-1. Caspase-11, the noncanonical inflammasome enzyme that recognizes LPS in cytosolic bacteria (7), was dispensable for cytokine release or inflammasome oligomerization upon *A. phagocytophilum* colonization of macrophages (Fig. 1A to D). Collectively, we detected endogenous NLRC4 inflammasome oligomerization in macrophages upon *A. phagocytophilum* stimulation. Although native inflammasome immunoblots were previously described (13, 15, 23), those studies used the HEK293T cell reconstitution system. We also provided strong evidence that the NLRC4 inflammasome in macrophages is critical for sensing *A. phagocytophilum* infection in the mammalian host. This was con-

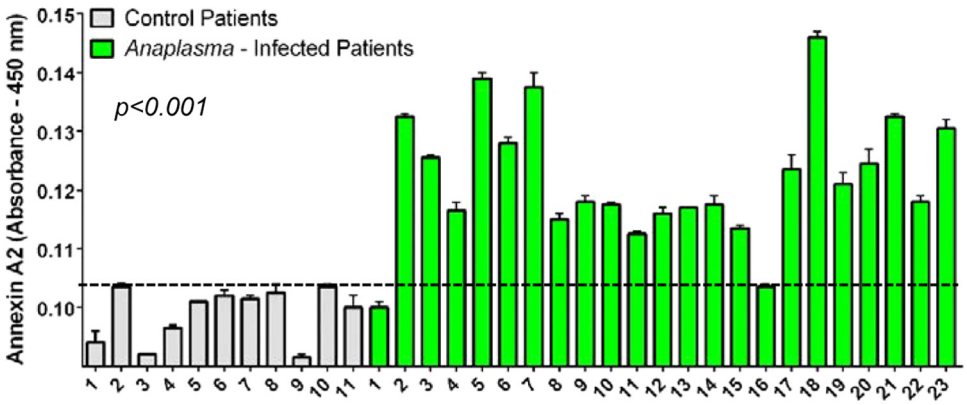

FIG 4 Sialostatin L2 binds better to sera of *A. phagocytophilum*-infected patients. Sialostatin L2 (200 ng) was immobilized on ELISA plates, and sera from 23 acutely infected and 11 control patients (1:5 dilution) were overlaid and probed against a human annexin A2 antibody. Absorbance values are shown after background subtraction. The *P* value was <0.05, as determined by ANOVA-Tukey test.

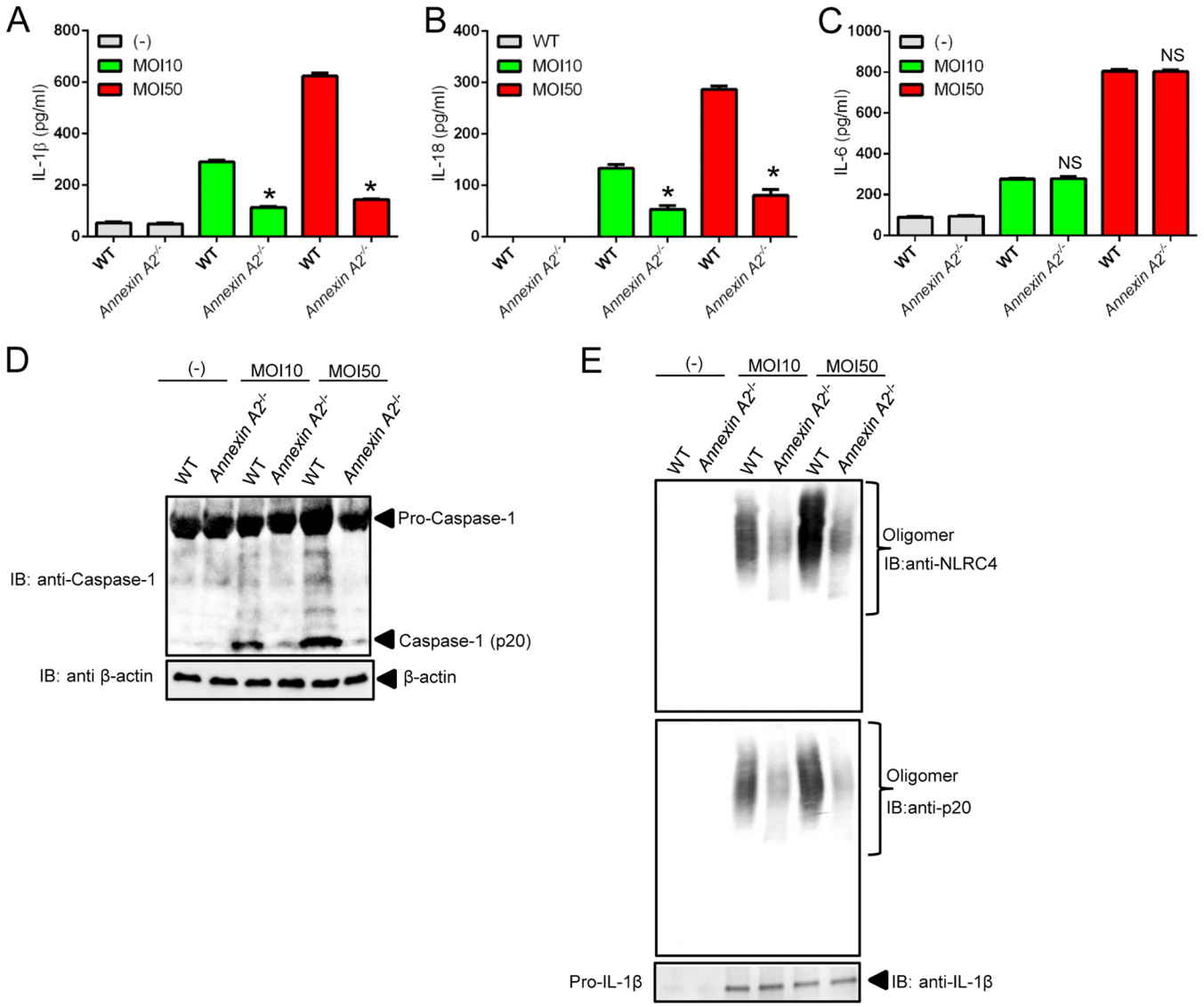

FIG 5 Annexin A2 affects the activity of the *A. phagocytophilum*-induced NLRC4 inflammasome. BMDMs were infected with *A. phagocytophilum* (MOI of 10 or 50). (A to C) IL-1β (A), IL-18 (B), and IL-6 (C) release measured by an ELISA. (D and E) Caspase-1 autoproteolysis (p20) (D) and NLRC4 and caspase-1 (p20) (E) native gel electrophoresis/immunoblotting (IB) of macrophages activated upon *A. phagocytophilum* infection. β-Actin and pro-IL-1β were detected in lysates. *, $P < 0.05$; NS, not significant (as determined by Student's *t* test). −, nonstimulated.

sistent with previous work correlating disease outcome with classical macrophage activation in both animal models and patients (16, 24–26).

Annexin A2 binds to the tick salivary protein sialostatin L2. Next, we demonstrated that in the presence of the tick salivary molecule sialostatin L2, *A. phagocytophilum* colonization of macrophages resulted in reduced caspase-1 activity and inflammation (16), suggesting that sialostatin L2 may interfere with the *A. phagocytophilum*-induced inflammasome. Here, macrophages were pretreated with recombinant sialostatin L2 (rSL2) prior to *A. phagocytophilum* colonization. rSL2 blocked NLRC4 oligomerization, and this effect was reversed when an anti-sialostatin L2 IgG-purified polyclonal antibody bound to rSL2 before macrophage exposure to this pathogen (Fig. 2A). We then used an unbiased pulldown assay followed by mass spectrometry and discovered that the phospholipid binding protein annexin A2 strongly bound to rSL2. To confirm these findings, we coincubated recombinant annexin A2 with rSL2 and performed mobility shift electrophoresis. The mobility of annexin A2 was shifted with increasing amounts of rSL2 (Fig. 2B). These results were substantiated by an ELISA-based assay (Fig. 2C). The binding of annexin A2 to rSL2 occurred regardless of which molecule was surface immobilized on the ELISA plate (see Fig. S1 in the supplemental material). Furthermore, the interaction of annexin A2 and rSL2 was blocked by a sialostatin L2-specific monoclonal antibody (see Fig. S2 in the supplemental material). The sialostatin L2 monoclonal antibody inhibited the binding of rSL2 to annexin A2 in a dose-dependent manner (Fig. 2D).

To validate these biochemical interactions, we prepared wild-type and *Annexin a2*$^{-/-}$ macrophages. rSL2 bound poorly to *Annexin a2*$^{-/-}$ macrophage lysates compared to wild-type cells, as judged by native gels and ELISAs (Fig. 2E and F). Finally, we per-

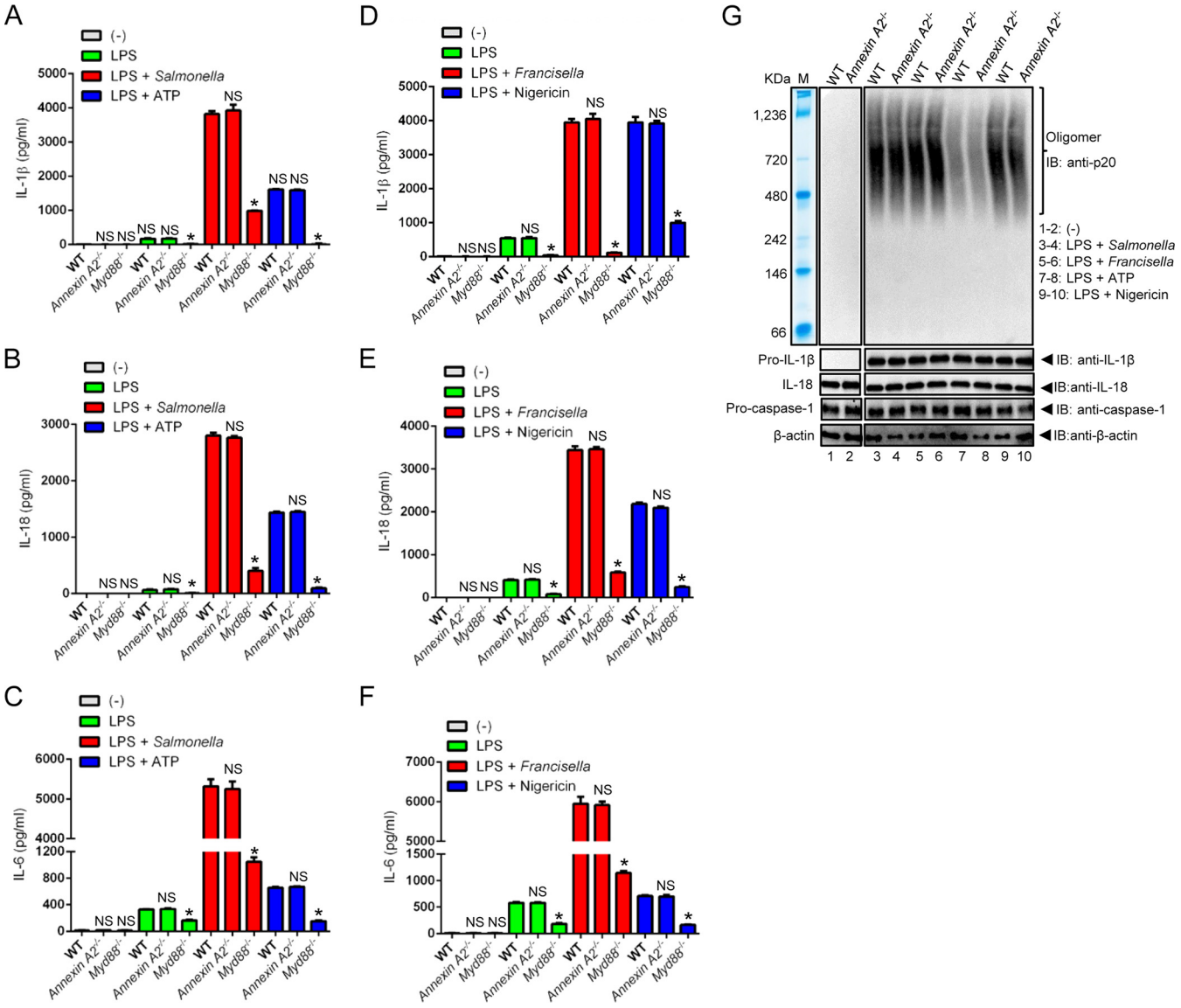

FIG 6 Annexin A2 deficiency does not affect canonical inflammasomes. (A to F) BMDMs primed with LPS (50 ng/ml) followed by infection with *Salmonella* (MOI of 25) or ATP stimulation (5 mM) (A to C) or infection with *Francisella* (MOI or 50) or nigericin stimulation (10 μM) (D to F). Shown are data from IL-1β (A and D), IL-18 (B and E), and IL-6 (C and F) ELISAs. (G) *Salmonella* (MOI of 25), ATP (5 mM), *Francisella* (MOI of 50), or nigericin (10 μM) stimulation of BMDMs and native immunoblotting (IB) of p20. β-Actin, pro-IL-1β, caspase-1, and pro-IL-18 were detected in lysates. *, $P < 0.05$; NS, not significant (as determined by ANOVA-Tukey test). −, nonstimulated. M, marker.

formed structural docking of sialostatin L2 to annexin A2 and predicted that loop 2, but not loop 1 or the N terminus of sialostatin L2, binds to annexin A2 (Fig. 3A). This model was experimentally verified by using peptides specific for each protein region. Only loop 2 of sialostatin L2 was bound to annexin A2 (Fig. 3B).

There is increasing evidence suggesting that the disease caused by *A. phagocytophilum* in patients is more complex than that in model systems (27). To provide translational relevance to our research findings, we determined whether rSL2 bound to human annexin A2 in a pathophysiological setting. We obtained sera from 23 acutely infected patients and compared the results to those for sera from 11 control individuals. Annexin A2 bound better to rSL2 in the sera of 21 out of 23 *A. phagocytophilum*-infected patients than in the sera of control individuals (Fig. 4).

Annexin A2 regulates the NLRC4 inflammasome pathway upon *A. phagocytophilum* infection. Subsequently, we investigated whether *Annexin a2*$^{-/-}$ macrophages had a defect in IL-1β and IL-18 secretion upon *A. phagocytophilum* colonization. Wild-type macrophages secreted significantly larger amounts of IL-1β and IL-18 at multiplicities of infection (MOI) of 10 and 50 than did *Annexin a2*$^{-/-}$ cells (Fig. 5A and B). This effect did not appear to be a global cytokine defect because there was no measurable difference in IL-6 levels between wild-type and *Annexin a2*$^{-/-}$ macrophages (Fig. 5C). *Annexin a2*$^{-/-}$ macrophages were also defective for caspase-1 activation and NLRC4 oligomerization (Fig. 5D and E). In contrast, *Annexin a2*$^{-/-}$ macrophages secreted IL-1β, IL-18, and IL-6 at wild-type levels when infected with *Salmonella*, a canonical NLRC4 agonist (Fig. 6A to C). Comparable results were also obtained with the NLRP3 agonists ATP and ni-

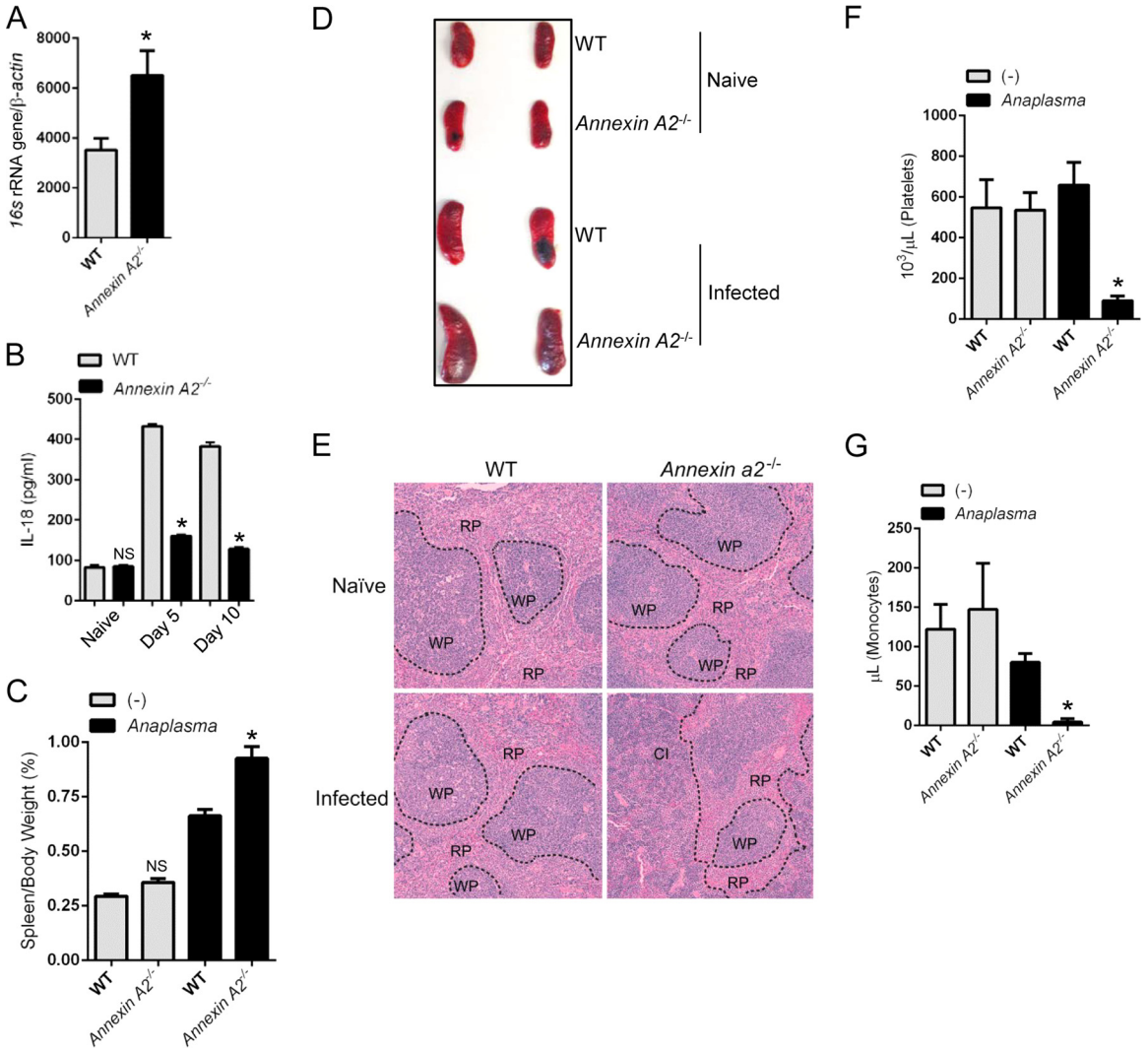

FIG 7 Annexin A2 restricts *A. phagocytophilum* infection *in vivo*. Shown are data for *A. phagocytophilum* infection of wild-type ($n = 20$) and *Annexin a2*$^{-/-}$ ($n = 11$) mice. (A) Bacterial load in the peripheral blood of infected mice. (B) IL-18 release in sera of infected animals. (C and D) Splenomegaly for *Annexin a2*$^{-/-}$ mice infected with *A. phagocytophilum*. (E) Splenic architecture depicting cellular infiltration (CI) in the red pulp (RP) and white pulp (WP) during *A. phagocytophilum* infection. (F and G) Thrombocytopenia (F) and monocytopenia (G) in *Annexin a2*$^{-/-}$ mice infected with *A. phagocytophilum*. *, $P < 0.05$; NS, not significant (as determined by ANOVA-Tukey test or Student's *t* test). −, naive animals.

gericin and the AIM2 stimulant *Francisella* (Fig. 6A to F). Not surprisingly, *Myd88*$^{-/-}$ macrophages exhibited defects in all parameters measured (Fig. 6A to F). Furthermore, *Salmonella*, *Francisella*, ATP, and nigericin induced inflammasome oligomerization independently of annexin A2 (Fig. 6G). Overall, we discovered that the signaling cascade that regulates the *A. phagocytophilum*-induced inflammasome is fundamentally different from other protein scaffolds, as annexin A2 was necessary for NLRC4 oligomerization upon *A. phagocytophilum* infection. Conversely, the assembly of canonical inflammasomes, here represented by the agonists *Salmonella*, *Francisella*, ATP, and nigericin, occurred regardless of the presence of annexin A2.

Annexin A2 deficiency renders susceptibility to *A. phagocytophilum* infection. To evaluate the biological impact of these biochemical interactions *in vivo*, we infected mice deficient in annexin A2 with *A. phagocytophilum*. Compared to *Nlrc4*$^{-/-}$ and *Caspase-1/11*$^{-/-}$ mice (17), *Annexin a2*$^{-/-}$ animals were susceptible to *A. phagocytophilum* infection (Fig. 7A). Moreover, mice deficient in annexin A2 showed a reduced release of IL-18 secretion in the peripheral blood compared to the wild-type genotype (Fig. 7B). These findings were consistent with our previous reports showing that IL-18 release mediated by the NLRC4 inflammasome regulates IFN-γ production by CD4$^+$ T cells upon *A. phagocytophilum* infection (17).

The *A. phagocytophilum* mouse model is characterized by splenomegaly and mild to severe inflammatory splenic histopathology (28). *Annexin a2*$^{-/-}$ mice revealed enlarged spleens compared to those of control animals (Fig. 7C and D). *Annexin a2*$^{-/-}$ animals also had increased cellular infiltration in the red pulp and damage to the splenic architecture upon *A. phagocytophilum* infection (Fig. 7E). Concurrently, thrombocytopenia and monocytopenia, two commonly observed clinical presentations during *A. phagocytophilum* infection (27), ensued in *Annexin a2*$^{-/-}$ mice (Fig. 7F and G).

In summary, we demonstrate in this report that (i) annexin A2 regulates the formation of the NLRC4 inflammasome during *A. phagocytophilum* infection, (ii) annexin A2 is critically important for *A. phagocytophilum* infection *in vivo*, (iii) sialostatin L2 binds to annexin A2 in both mice and humans, and (iv) sialostatin L2 inhibits the activation of mouse NLRC4 inflammasome formation upon rickettsial infection. The implications for these findings are wide in scope, as ticks, mosquitoes, biting flies, fleas, and blood-feeding bugs secrete salivary proteins for modulating host defenses. Intriguingly, our report also suggests the possibility that an alternative signaling cascade for the inflammasome may exist, because unlike *Salmonella*, *A. phagocytophilum* does not have the NLRC4 canonical activators (29).

ACKNOWLEDGMENTS

We acknowledge Vishva Dixit (Genentech) for providing anti-caspase-1 antibody and *Caspase-11*$^{-/-}$ mice; Stefanie Vogel (University of Maryland, Baltimore) for providing strains of *Salmonella* and *Francisella*; Katherine A. Hajjar (Weill Cornell Medical College) for providing the *Annexin a2*$^{-/-}$ mice; the Core facilities at the University of Maryland, Baltimore, for services related to proteomics and pathology; and Hal Neely, Martin Flajnik, and Vickie Knepper-Adrian for technical assistance.

We declare no competing financial interests.

This work was supported by the University of Maryland, Baltimore, School of Medicine.

FUNDING INFORMATION

This work, including the efforts of Joao H. F. Pedra, was funded by HHS | NIH | National Institute of Allergy and Infectious Diseases (NIAID) (R01 AI093653). This work, including the efforts of Joao H. F. Pedra, was funded by HHS | NIH | National Institute of Allergy and Infectious Diseases (NIAID) (R01 AI116523).

The funders had no role in study design, data collection and interpretation, or the decision to submit the work for publication.

REFERENCES

1. **Fontaine A, Diouf I, Bakkali N, Misse D, Pages F, Fusai T, Rogier C, Almeras L.** 2011. Implication of haematophagous arthropod salivary proteins in host-vector interactions. Parasit Vectors **4:**187. http://dx.doi.org/10.1186/1756-3305-4-187.
2. **Chmelar J, Kotal J, Karim S, Kopacek P, Francischetti IM, Pedra JH, Kotsyfakis M.** 2016. Sialomes and mialomes: a systems-biology view of tick tissues and tick-host interactions. Trends Parasitol **32:**242–254. http://dx.doi.org/10.1016/j.pt.2015.10.002.
3. **Kotal J, Langhansova H, Lieskovska J, Andersen JF, Francischetti IM, Chavakis T, Kopecky J, Pedra JH, Kotsyfakis M, Chmelar J.** 2015. Modulation of host immunity by tick saliva. J Proteomics **128:**58–68. http://dx.doi.org/10.1016/j.jprot.2015.07.005.
4. **Sakhon OS, Severo MS, Kotsyfakis M, Pedra JH.** 2013. A Nod to disease vectors: mitigation of pathogen sensing by arthropod saliva. Front Microbiol **4:**308. http://dx.doi.org/10.3389/fmicb.2013.00308.
5. **Bernard Q, Jaulhac B, Boulanger N.** 2014. Smuggling across the border: how arthropod-borne pathogens evade and exploit the host defense system of the skin. J Investig Dermatol **134:**1211–1219. http://dx.doi.org/10.1038/jid.2014.36.
6. **Wikel S.** 2013. Ticks and tick-borne pathogens at the cutaneous interface: host defenses, tick countermeasures, and a suitable environment for pathogen establishment. Front Microbiol **4:**337. http://dx.doi.org/10.3389/fmicb.2013.00337.
7. **Guo H, Callaway JB, Ting JP.** 2015. Inflammasomes: mechanism of action, role in disease, and therapeutics. Nat Med **21:**677–687. http://dx.doi.org/10.1038/nm.3893.
8. **Lage SL, Longo C, Branco LM, da Costa TB, Buzzo CDL, Bortoluci KR.** 2014. Emerging concepts about NAIP/NLRC4 inflammasomes. Front Immunol **5:**309. http://dx.doi.org/10.3389/fimmu.2014.00309.
9. **Vance RE.** 2015. The NAIP/NLRC4 inflammasomes. Curr Opin Immunol **32:**84–89. http://dx.doi.org/10.1016/j.coi.2015.01.010.
10. **Zhang L, Chen S, Ruan J, Wu J, Tong AB, Yin Q, Li Y, David L, Lu A, Wang WL, Marks C, Ouyang Q, Zhang X, Mao Y, Wu H.** 2015. Cryo-EM structure of the activated NAIP2-NLRC4 inflammasome reveals nucleated polymerization. Science **350:**404–409. http://dx.doi.org/10.1126/science.aac5789.
11. **Hu Z, Zhou Q, Zhang C, Fan S, Cheng W, Zhao Y, Shao F, Wang HW, Sui SF, Chai J.** 2015. Structural and biochemical basis for induced self-propagation of NLRC4. Science **350:**399–404. http://dx.doi.org/10.1126/science.aac5489.
12. **Zhao Y, Yang J, Shi J, Gong YN, Lu Q, Xu H, Liu L, Shao F.** 2011. The NLRC4 inflammasome receptors for bacterial flagellin and type III secretion apparatus. Nature **477:**596–600. http://dx.doi.org/10.1038/nature10510.
13. **Kofoed EM, Vance RE.** 2011. Innate immune recognition of bacterial ligands by NAIPs determines inflammasome specificity. Nature **477:**592–595. http://dx.doi.org/10.1038/nature10394.
14. **Rayamajhi M, Zak DE, Chavarria-Smith J, Vance RE, Miao EA.** 2013. Mouse NAIP1 detects the type III secretion system needle protein. J Immunol **191:**3986–3989. http://dx.doi.org/10.4049/jimmunol.1301549.
15. **Yang J, Zhao Y, Shi J, Shao F.** 2013. Human NAIP and mouse NAIP1 recognize bacterial type III secretion needle protein for inflammasome activation. Proc Natl Acad Sci U S A **110:**14408–14413. http://dx.doi.org/10.1073/pnas.1306376110.
16. **Chen G, Wang X, Severo MS, Sakhon OS, Sohail M, Brown LJ, Sircar M, Snyder GA, Sundberg EJ, Ulland TK, Olivier AK, Andersen JF, Zhou Y, Shi GP, Sutterwala FS, Kotsyfakis M, Pedra JH.** 2014. The tick salivary protein sialostatin L2 inhibits caspase-1-mediated inflammation during *Anaplasma phagocytophilum* infection. Infect Immun **82:**2553–2564. http://dx.doi.org/10.1128/IAI.01679-14.
17. **Pedra JH, Sutterwala FS, Sukumaran B, Ogura Y, Qian F, Montgomery RR, Flavell RA, Fikrig E.** 2007. ASC/PYCARD and caspase-1 regulate the IL-18/IFN-γ axis during *Anaplasma phagocytophilum* infection. J Immunol **179:**4783–4791. http://dx.doi.org/10.4049/jimmunol.179.7.4783.
18. **Scharf B, Clement CC, Wu XX, Morozova K, Zanolini D, Follenzi A, Larocca JN, Levon K, Sutterwala FS, Rand J, Cobelli N, Purdue E, Hajjar KA, Santambrogio L.** 2012. Annexin A2 binds to endosomes following organelle destabilization by particulate wear debris. Nat Commun **3:**755. http://dx.doi.org/10.1038/ncomms1754.
19. **Tennant SM, Wang JY, Galen JE, Simon R, Pasetti MF, Gat O, Levine MM.** 2011. Engineering and preclinical evaluation of attenuated nontyphoidal *Salmonella* strains serving as live oral vaccines and as reagent strains. Infect Immun **79:**4175–4185. http://dx.doi.org/10.1128/IAI.05278-11.
20. **Tovchigrechko A, Vakser IA.** 2006. GRAMM-X public Web server for protein-protein docking. Nucleic Acids Res **34:**W310–W314. http://dx.doi.org/10.1093/nar/gkl206.
21. **Pierce BG, Wiehe K, Hwang H, Kim BH, Vreven T, Weng Z.** 2014. ZDOCK server: interactive docking prediction of protein-protein complexes and symmetric multimers. Bioinformatics **30:**1771–1773. http://dx.doi.org/10.1093/bioinformatics/btu097.
22. **Baugh EH, Lyskov S, Weitzner BD, Gray JJ.** 2011. Real-time PyMOL visualization for Rosetta and PyRosetta. PLoS One **6:**e21931. http://dx.doi.org/10.1371/journal.pone.0021931.
23. **Tenthorey JL, Kofoed EM, Daugherty MD, Malik HS, Vance RE.** 2014. Molecular basis for specific recognition of bacterial ligands by NAIP/NLRC4 inflammasomes. Mol Cell **54:**17–29. http://dx.doi.org/10.1016/j.molcel.2014.02.018.
24. **Lepidi H, Bunnell JE, Martin ME, Madigan JE, Stuen S, Dumler JS.** 2000. Comparative pathology, and immunohistology associated with clinical illness after *Ehrlichia phagocytophila*-group infections. Am J Trop Med Hyg **62:**29–37.
25. **Dumler JS, Barat NC, Barat CE, Bakken JS.** 2007. Human granulocytic anaplasmosis and macrophage activation. Clin Infect Dis **45:**199–204. http://dx.doi.org/10.1086/518834.
26. **Choi KS, Scorpio DG, Dumler JS.** 2004. *Anaplasma phagocytophilum* ligation to Toll-like receptor (TLR) 2, but not to TLR4, activates macrophages for nuclear factor-κB nuclear translocation. J Infect Dis **189:**1921–1925. http://dx.doi.org/10.1086/386284.
27. **Bakken JS, Dumler JS.** 2015. Human granulocytic anaplasmosis. Infect Dis Clin North Am **29:**341–355. http://dx.doi.org/10.1016/j.idc.2015.02.007.

28. **Choi KS, Scorpio DG, Dumler JS.** 2014. Stat1 negatively regulates immune-mediated injury with *Anaplasma phagocytophilum* infection. J Immunol **193:**5088–5098. http://dx.doi.org/10.4049/jimmunol.1401381.
29. **Dunning Hotopp JC, Lin M, Madupu R, Crabtree J, Angiuoli SV, Eisen JA, Seshadri R, Ren Q, Wu M, Utterback TR, Smith S, Lewis M, Khouri H, Zhang C, Niu H, Lin Q, Ohashi N, Zhi N, Nelson W, Brinkac LM, Dodson RJ, Rosovitz MJ, Sundaram J, Daugherty SC, Davidsen T, Durkin AS, Gwinn M, Haft DH, Selengut JD, Sullivan SA, Zafar N, Zhou L, Benahmed F, Forberger H, Halpin R, Mulligan S, Robinson J, White O, Rikihisa Y, Tettelin H.** 2006. Comparative genomics of emerging human ehrlichiosis agents. PLoS Genet **2:**e21. http://dx.doi.org/10.1371/journal.pgen.0020021.